Reversible Ammonia Sorption for the Primary Life Support System (PLSS)

Marek A. Wójtowicz[1], Joseph E. Cosgrove[2], Michael A. Serio[3]
Advanced Fuel Research, Inc., East Hartford, CT, 06108

and

Mallory A. Jennings[4]
NASA Johnson Space Center, Houston, TX 77058

Results are presented on the development of regenerable trace-contaminant (TC) sorbent for use in Extravehicular Activities (EVAs), and more specifically in the Primary Life Support System (PLSS). Since ammonia is the most important TC to be captured, data presented in this paper are limited to ammonia sorption, with results relevant to other TCs to be reported at a later time. The currently available TC-control technology involves the use of a packed bed of acid-impregnated granular charcoal. The sorbent is non-regenerable, and its use is associated with appreciable pressure drop, i.e. power consumption. The objective of this work is to demonstrate the feasibility of using vacuum-regenerable sorbents for PLSS application. In this study, several carbon sorbent monoliths were fabricated and tested. Multiple adsorption/vacuum-regeneration cycles were demonstrated at room temperature, as well as carbon surface conditioning that enhances ammonia sorption without impairing sorbent regeneration. Depending on sorbent monolith geometry, the reduction in pressure drop with respect to granular sorbent was found to be between 50% and two orders of magnitude. Resistive heating of the carbon sorbent monolith was demonstrated by applying voltage to the opposite ends of the monolith.

Nomenclature

AFR = Advanced Fuel Research, Inc.
BET = Brunauer, Emmett, and Teller
DFT = Density Functional Theory
D-R = Dubinin-Radushkevich
EVA = Extravehicular Activity
FTIR = Fourier Transform Infrared
MGA = Multi-Gas Analyzer
MCT = mercury-cadmium-telluride
NASA = National Aeronautics and Space Administration
NMP = N-Methylpyrrolidone
PLSS = Primary Life Support System
PVDC = polyvinylidene chloride
RVC = reticulated vitreous carbon
TC = Trace Contaminant
TCCS = Trace Contaminant Control System

[1] Vice President, Clean Energy & Carbon Materials, Advanced Fuel Research, Inc., 87 Church St., E. Hartford, CT 06108.
[2] Laboratory Manager, Advanced Fuel Research, Inc., 87 Church Street, East Hartford, CT 06108.
[3] President, Advanced Fuel Research, Inc., 87 Church Street, East Hartford, CT 06108.
[4] PLSS Trace Contaminant Control Lead, NASA Johnson Space Center, EC5 - Space Suit & Crew Survival Systems, Houston, TX 77058.

I. Introduction

THE NASA objective of expanding the human experience into the far reaches of space requires the development of regenerable life support systems. This study addresses the development of a regenerable air-revitalization system for trace-contaminant (TC) removal for the space suit used in Extravehicular Activities (EVAs). Currently, a bed of granular activated carbon is used for TC control. The carbon is impregnated with phosphoric acid to enhance ammonia sorption, but this also makes regeneration difficult, if not impossible. Temperatures as high as 200 °C have been shown to be required for only partial desorption of ammonia on time scales of 18–140 hours[1]. Neither these elevated temperatures nor the long time needed for sorbent regeneration are acceptable. Thus, the activated carbon has been treated as an expendable resource and the sorbent bed has been oversized in order to last throughout the entire mission [23 kg carbon for cabin-air revitalization and about 1 lb (0.454 kg) for the space suit]. Another important consideration is pressure drop. Granular sorbent offers significant resistance to gas flow, which is associated with a high demand for fan power. Thus, there is a great need for an effective TC sorbent that could be regenerated by short exposure to vacuum at low temperatures (under 80 °C for less than 1 hour). A monolithic structure (e.g., a honeycomb) is also desired to reduce fan-power consumption.

The current state of the art and historical approaches to trace-contaminant removal in the primary life support system (PLSS), often referred to as the space suit backpack, were recently reviewed by Paul and Jennings[1]. Activated carbon (charcoal) was identified as a clear winner for the trace contaminant control system (TCCS) application in terms of effectiveness, simplicity, and maturity of this technological solution. Carbon regeneration, however, has always been problematic, mainly because all carbons used to date were impregnated with phosphoric acid or other acidic compounds. This results in a virtually irreversible chemical reaction with ammonia and salt formation, which greatly complicates regeneration. It has been widely believed that unimpregnated carbon does not adsorb ammonia (see, for example, Ref. 2–4), and that chemisorption is the only option to bind ammonia to the carbon surface. We believe this is true only for carbons with a fairly wide distribution of pore sizes, i.e. for almost all commercial carbons. If the pore size could be optimized, however, in such a way so that almost all pores have the right size for ammonia physisorption, it is our belief that no chemical impregnation would be necessary to effect ammonia sorption. Furthermore, physisorbed ammonia should be relatively easy to desorb using vacuum regeneration as no chemical bonds would have to be broken. We are unaware, however, of any systematic studies that address the effect of carbon pore structure on the regeneration performance of trace-contaminant sorbents.

We believe that a non-optimal sorbent structure, both internal (pore-size distribution) and external (intraparticle heat transfer limitations), combined with chemical impregnation, has led to extremely long sorbent regeneration time scales on the order of 5–140 hours depending on temperature (130–200 °C)[1]. In this study, we examine the use of monolithic carbon structures optimized with respect to TC desorption rates as a function of temperature, pressure (vacuum), and humidity. The main focus of the project is vacuum regeneration, but rapid resistive heating to moderately low temperatures (up to 80 °C) should also be considered as an optional feature that accelerates the vacuum regeneration process.

We believe that good TC-sorption capacity can be accomplished through the combination of a particularly favorable pore structure for optimum physical adsorption (physisorption) of TCs, and surface conditioning that enhances adsorption without adversely affecting vacuum regeneration. The avoidance of acid impregnation of carbon further helps the cause of adsorption reversibility. Finally, the issue of pressure drop and fan-power requirement is addressed through the use of a monolithic sorbent structure.

The objective of this work is to demonstrate the feasibility of using vacuum-regenerable sorbents for PLSS application. The innovations explored in this study are: (1) vacuum (or vacuum/thermal) regenerable operation, in contrast to the currently used bed of expendable sorbent; (2) TC removal based on *reversible physisorption* on high-purity carbon rather than on *irreversible chemisorption* on activated carbon impregnated with acidic compounds; (3) a carbon monolith sorbent, in contrast to the currently used bed of granular charcoal; (4) carbon surface conditioning (oxidation) to enhance TC sorption without adversely affecting sorbent regeneration; (5) low pressure drop; (6) carbon pore structure tailored for optimal vacuum/thermal regeneration; (7) resistive heating of the carbon monolith for rapid regeneration; and (8) good resistance to dusty environments.

II. Materials and Experimental Techniques

A. Carbon Monolith Preparation

1. Monoliths with Parallel Channels

In general, monolithic carbon sorbents can be produced by carbonization of monolithic, polymer-based precursors, which is followed by carbon activation to develop surface area. A novel carbon-activation method and carbon monolith preparation techniques were previously used at Advanced Fuel Research, Inc. (AFR) to control the micropore structure of the carbon sorbent. This methodology was originally developed in a NASA-funded project on hydrogen storage using microporous carbons[5-9]. Other publications on this technology include Ref. 10-16. Another related NASA project was on the use of carbon monolithic supports in combination with liquid amines to provide effective CO_2 removal[17-19]. Examples of microporous carbon monoliths fabricated at AFR are shown in Figure 1. Other designs, e.g., a honeycomb configuration, are of course possible, and the artifacts presented in Figure 1 are shown merely to illustrate the concept. The reader is referred to the cited literature for the description of monolith fabrication. Polyvinylidene chloride (PVDC) is known to produce almost entirely microporous carbon upon carbonization (pore sizes < 20 Å), and this is why this polymer is particularly suitable for adsorption of volatile compounds. Two PVDC carbon monoliths from our previous project were used for ammonia-sorption tests. They are shown in Figure 1, and details of their preparation can be found in Ref. 17. Each monolith had 121 channels, one of them was unactivated, and the other one was CO_2 activated to about 20% weight loss.

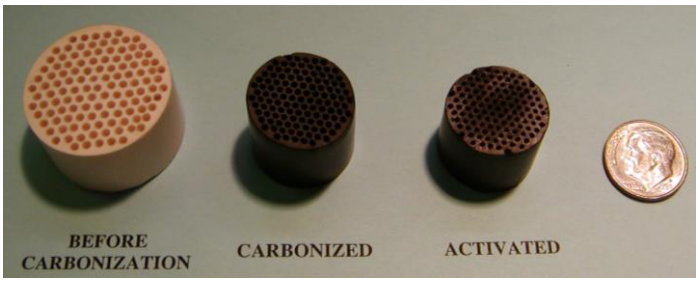

Figure 1. A monolith fabricated at AFR from the polyvinylidene chloride (PVDC) precursor before carbonization, carbonized, and activated[17,18].

2. Vitreous Carbon Foam Monoliths

Most effort in this study went into the development of a novel methodology for making PVDC-based carbon that has the structure provided by the skeleton made from vitreous carbon foam. A low-density support structure was coated with a PVDC precursor and carbonized to form a porous sorbent-coated monolith. The objective was to produce predominantly microporous monolithic carbon (from PVDC) that had good mechanical properties (from vitreous carbon foam). These structures were expected to show good NH_3 absorption and desorption performance as well as low pressure drop.

The support structure that we employed was a Duocel® foam manufactured by ERG Aerospace Corporation. This foam is described as an open-cell, porous structure consisting of an interconnected network of solid "struts." It is available in a variety of pore sizes, defined as pores per inch (ppi), ranging from 5–100 ppi. Materials include aluminum, copper, reticulated vitreous carbon (RVC) and silicon carbide (SiC), and blocks of these materials can be obtained with volumes as high as 1.3 cu. ft. (carbon and silicon carbide). For the space-suit application, we chose to work with vitreous carbon as the sorbent support structure. Unlike the metal foam materials, vitreous carbon is chemically resistant to the HCl vapors that are evolved during carbonization of PVDC. Compared to SiC, the carbon foam is more readily available, has a lower cost, and is lighter for a given porosity. The 30–80 ppi foam used in this work is available as 4 x 4 inch panels in nominal thicknesses up to 0.5 inch. It was found that it could be easily and reproducibly cut into cylinders using a precision arch punch.

Two fabrication routes for producing the PVDC carbon-coated foam structures were explored. We first investigated a wet deposition technique in which the RVC foam substrates were dip-coated in a PVDC solution precursor and then carbonized. In the second approach, the foam substrates were filled with the dry PVDC powder and then carbonized. Three PVDC precursor powders were evaluated including a PVDC homopolymer from Honeywell, a Dow Chemical copolymer (Saran 506), and a Solvay Advanced Polymers copolymer (IXAN SGA-1). The main processing parameters that were investigated included the effects of carbonization temperature and the effects of activation on the ammonia adsorption performance. We also explored the effects of a carbon surface conditioning step using thermal oxidation in air. Experimental details for each fabrication method, surface conditioning and the ammonia adsorption testing and regeneration testing are provided below.

Solution Coating – For dip-coating experiments, RVC foam samples with pore sizes ranging from 30–80 ppi were cut into 22 mm diameter x 12 mm thick substrates. The mass of the bare substrates ranged from 0.2–0.25 g, depending on the pore size. The process of coating the substrates using a PVDC liquid precursor involved three basic steps, as illustrated in Figure 2. The foam samples were first dipped in a solution of PVDC/solvent and then briefly drained. In the second step the samples were submerged in a bath of hot water (40–50 °C) for a period of ~30 seconds, and then cured for 12–36 hours. The samples were then heat-treated in a pre-heated tube furnace at ~300 °C (Step 3) under flowing high purity nitrogen (1 L/min) to boil off any trapped solvent and water to partially carbonize the PVDC. To increase the mass of PVDC carbon in the foam, the process cycle was repeated, until the desired PVDC carbon/foam mass ratio was achieved. At this point, the samples were subjected to a final high temperature heat treatment (in nitrogen) to fully carbonize the PVDC. A heating rate of ~10 K/min was used up to 750 °C and ~15 K/min from 750 °C to the final cure temperature, up to 1050 °C. After the final high temperature carbonization step, mass of PVDC carbon deposited on the foam samples was found to be ~0.15–0.3 g/coat cycle, depending on the foam pore size and the PVDC solution concentration.

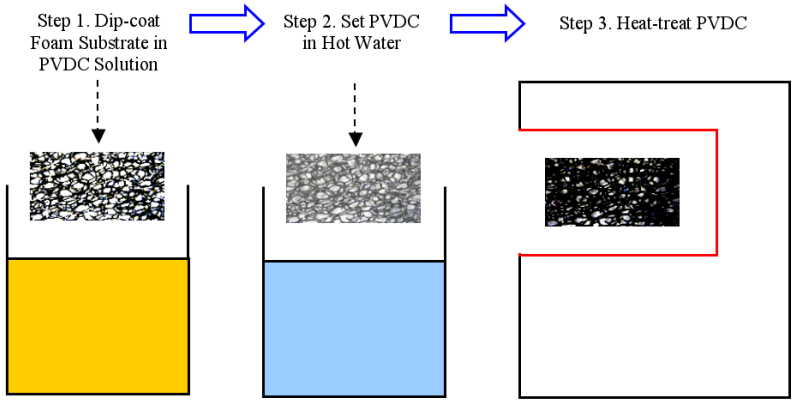

Figure 2. A single-cycle process sequence for PVDC coating of vitreous carbon foam.

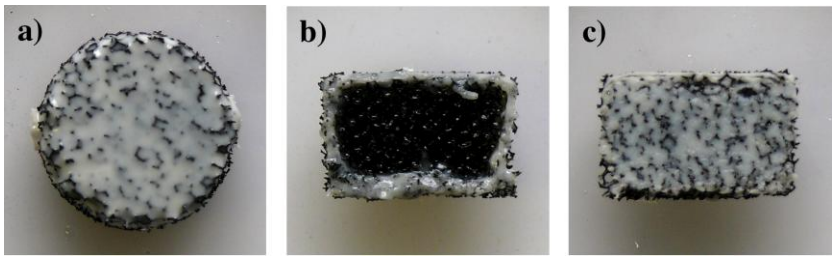

Figure 3. (a) Top-view (base) of a 30 ppi foam sample (22 mm in diameter) after a 30 second dip step in hot water; (b) Cross-sectional view of a 30 ppi foam sample immediately after a 30 second dip in hot water; (c) Cross-sectional view of a 30 ppi foam sample after a 30 second dip in hot water followed by an about 16-hour curing period in air. (Note: 3 different samples are shown.)

The PVDC precursor solutions (Step 1) were prepared by dissolving the PVDC powder in a suitable organic solvent, using vigorous stirring and modest heating to 50 °C. Of the three polymer formulations studied, the Solvay blend was the most soluble, in that it readily dissolved in acetone, methyl ethyl ketone and N-Methylpyrrolidone (NMP). The Solvay solutions were also observed to be the most stable, having shelf lives of more than one week for NMP-based solutions prepared up to 35% in concentration (by weight). The Dow PVDC blend was only soluble in NMP at concentrations up to 30% and its shelf life was limited to one day. The Honeywell homopolymer was much more difficult to dissolve, requiring heating to 100 °C and higher. However, upon cooling to below 50 °C, the solutions gelled and were unusable for dip-coating. Consequently, dip-coating of the RVC foams was only performed using the Solvay and Dow solutions.

The water submersion step (Step 2) partially crystallizes or "sets" the PVDC, forming a continuous external skin of polymer on the foam substrate, as shown in Figure 3a. (We cannot rule out that some type of reaction with the water is occurring, but it is more likely that that the water simply displaces the solvent, causing the PVDC to locally re-crystallize.) The outer skin seems to encapsulate the PVDC solution inside the foam matrix (Figure 3b), minimizing further drainage of the PVDC solution. After an additional curing period (> 12 hours) in air, a substantial amount of the PVDC inside the foam matrix is crystallized, as shown in Figure 3c. Note, however, that although in Figure 3c the foam/polymer structure appears completely solidified, there is still a significant amount of liquid that remains, including the solvent and possibly trapped water.

An important goal of the solution-coating method is that the coated sorbent has good adhesion to the carbon support structure. Figure 4 compares scanning electron microscopy (SEM) images obtained for an uncoated carbon foam disk and two different regions of a carbon foam disk after 5-coat cycles. For the uncoated sample (Figure 4a), the lattice nature of the foam is clearly evident in the image as several levels of the carbon framework can be seen. Figure 4b displays an image obtained from the external surface (base) of the coated disk. After five coating cycles, the carbon struts appear thicker and obviously coated, yet the underlying lattice is still evident. To further probe this sample, we sliced it in half (perpendicular to the cylinder axis) for SEM analysis of the inner coated region. As shown in Figure 4c, the carbon lattice is still evident but appears heavily coated, similar to the external surface of the sample.

Dry Powder Coating – The second PVDC carbon coating method that was studied used dry PVDC powder precursors. For these experiments, the substrates were cut from 80 ppi RVC foam into 22 mm diameter x 12 mm thick substrates. They were then placed into a sealed plastic container, partially filled with PVDC powder (Honeywell or Dow), and then gently shaken for a period of a few minutes. The powder-filled foam samples were then carbonized (in nitrogen), again in two separate heat treatments. Here, however, a ramp rate of 1 K/min was employed for the low temperature carbonization step to 300 °C to avoid "foaming". For the final heat-treatment step, a heating rate of ~1 K/min was used up to 550 °C and ~5 K/min from 550 °C to the final cure temperature (800–1450 °C). In these experiments, only the Honeywell and Dow PVDC powders were studied and only one carbon deposition cycle was performed for each sample. The yield of carbon for each sample was 0.5–0.6 g per run, which was much higher than the carbon yield per cycle for the dip-coated samples.

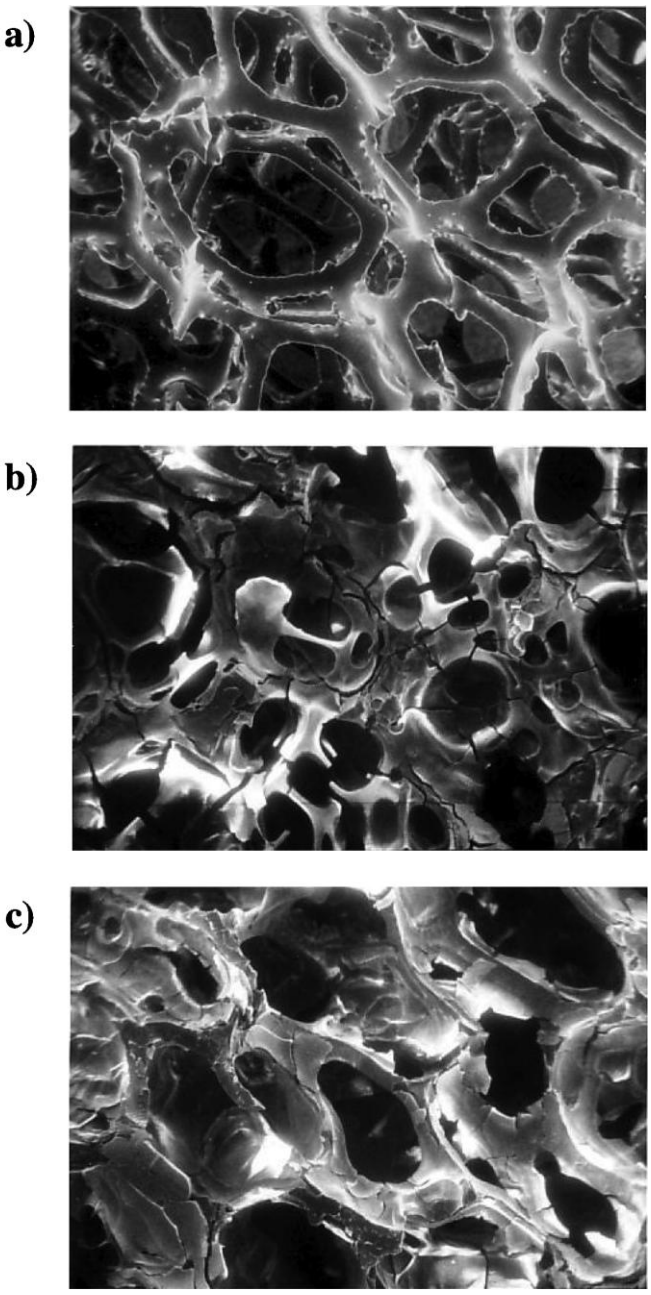

Figure 4. SEM images of: (a) an uncoated 30 ppi carbon foam cylinder; (b) the top surface of a 30 ppi foam cylinder after 5 coat cycles (net weight gain of 0.756 g) using a 19 wt% solution precursor; and (c) the middle region of the same coated cylinder sample.

CO_2 Activation – High-temperature activation of both dip-coated and dry-coated foam samples was performed in pure carbon dioxide, using a high-temperature tube furnace. The samples were heated to 900 °C at a ramp rate of ~22 K/min and held for 4 hours, yielding a burn-off of ~25%. We also observed similar burn-off in the RVC foam substrate and, therefore, always included a bare foam sample during each activation run, to correct for any foam losses in the PVDC carbon coated samples.

Thermal Oxidation – As described below, surface conditioning of the PVDC carbon after carbonization, via thermal oxidation at relatively modest temperatures, had a dramatic effect on ammonia adsorption. For these experiments, the PVDC carbon-coated foam samples were oxidized in ambient air at temperatures ranging from 250 °C to 325 °C for periods of up to 72 hours. At 250 °C, none of the samples that were studied showed any

weight loss after oxidation. At 325 °C, however, a sample carbonized to 900 °C showed ~20% burn-off, while a sample carbonized to 1450 °C showed no measurable weight loss.

B. Granular Activated Carbons

Three types of commercially available granular activated carbons were obtained for the project from the leading activated-carbon manufacturers: Calgon and Norit. We asked Calgon to provide us with what they deemed to be their best carbon for ammonia sorption: one acid-treated and one non-impregnated. In response to our request, Calgon supplied us with Ammonasorb II (impregnated with phosphoric acid), and BPL (no acid impregnation or acid washing). We also used Norit DARCO, which is produced from lignite coal by steam activation, followed by acid wash. All the above activated carbons were ground to –30+40 mesh size prior to ammonia-sorption testing.

C. Carbon Characterization

A fully automated gas-sorption system Quantachrome ASiQwin was used for collecting and processing nitrogen-isotherm data. Several carbon-microlith samples were tested, and all samples were outgassed under vacuum at 300 ºC for at least 3 hours prior to measurements. Nitrogen adsorption isotherms were then determined at 77 K, and these data were used to perform the following analyses: (a) BET surface area; (b) pore volume; (c) Dubinin-Radushkevich (D-R) micropore surface area and micropore volume; and (d) pore-size distribution of micropores using the Density Functional Theory (DFT). Where appropriate, the pore-size distribution in the mesopore region was also calculated using the BJH approach.

D. Ammonia Sorption and Sorbent Regeneration

A test stand for ammonia adsorption measurements under dry and humid conditions was assembled, as shown schematically in Figure 5. The test stand was used to evaluate the PVDC carbon monoliths as well as three granular commercial activated carbon sorbents, including Calgon's Ammonasorb II phosphoric acid-impregnated formulation. The apparatus, shown in Figure 5, incorporates a Fourier transform infrared (FTIR) spectrometer-based On-Line Technologies model 2010 Multi-Gas Analyzer (MGA) for both the NH_3 and H_2O quantification. Using mass flow controllers, a 120 ppm NH_3/N_2 gas mixture is mixed with a 35% O_2/N_2 blend to achieve the desired concentration of NH_3 in a balance of O_2 and N_2. For humidifying the gas stream, a portion of the O_2/N_2 mixture is re-routed through a water bubbler, using fine needle valves for adjustment. During testing, the final mixture is first routed through a sample bypass line, to establish the baseline NH_3 and humidity conditions. The gas is then re-directed through the sample "cell" for the sorbent adsorption testing. The sample cell consists of a quartz or glass tube that contains the sorbent sample. It is mounted in a vertical orientation with the gas inlet at the top of the cell so that gas flow is in a downward direction.

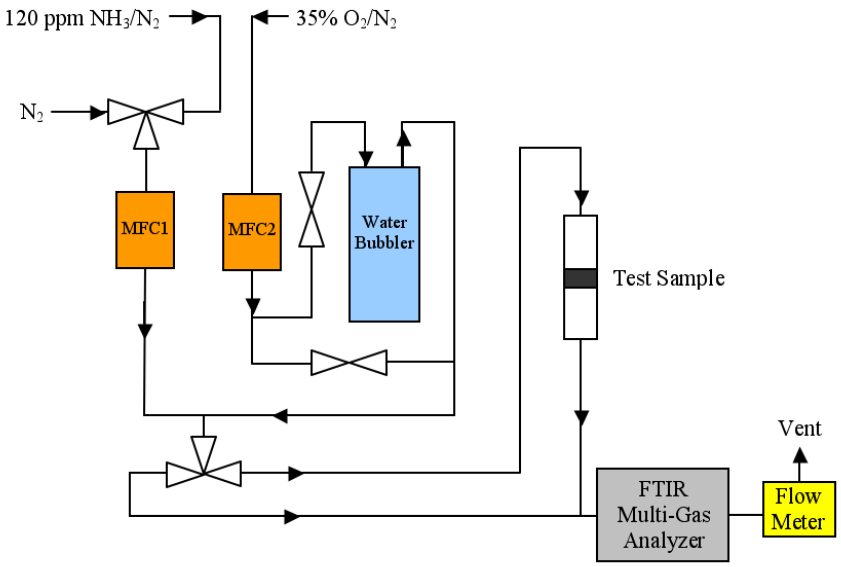

Figure 5. A schematic representation of the ammonia sorption/desorption test apparatus.

The 22 mm diameter PVDC carbon-coated foam samples, and also multi-channel carbon monoliths, were wrapped in Teflon tape and then inserted into a 22 mm diameter quartz tube. The carbon sample height was typically 1.2 cm. The Teflon tape assures a snug and reasonably gas-tight fit between the foam sample and the quartz tubing. For the granular sorbents, ~0.25 g of sieved sample (+40-30 mesh) was loaded into 5 mm i.d. glass

tubes and held in place using ceramic wool on both ends, resulting in a carbon bed length of about 15 mm. For the monolith samples, the inlet NH_3 concentration and flow rate were 20 ppm and 1 L/min, respectively. For the granular samples, the inlet concentration and flow rate were 23 ppm and 0.45 L/min.

The MGA shown in Figure 5 employs a liquid nitrogen-cooled, mercury-cadmium-telluride (MCT) detector with a bandpass of 500–6500 cm^{-1} and a spectral resolution of 0.5 cm^{-1}. The instrument employs a heated, multi-pass gas sampling cell with an effective pathlength of 5.1 m. The long effective pathlength and the high resolution of the instrument enable sub-ppm sensitivity to NH_3, even in the presence of high H_2O concentrations. All data were collected at one minute intervals. The procedure was to monitor the NH_3 breakthrough curves (NH_3 concentration vs time) and to terminate the adsorption measurement when the NH_3 concentration had reached 90% of the cell inlet concentration (after breakthrough).

Two methods of sorbent regeneration were explored: nitrogen gas desorption and vacuum desorption, with and without mild heating (~60 °C). The procedure for nitrogen desorption was to switch the sample gas flow to pure N_2, after the NH_3 adsorption measurement was completed, and to monitor the NH_3 desorption using the MGA. For vacuum regeneration experiments, the sample cell was removed from the test stand and installed in a high vacuum chamber pumped by a turbomolecular pump (base vacuum of ~10^{-6} Torr). After the vacuum regeneration, the sample cell was re-installed on the test stand and the NH_3 adsorption was measured again to determine the regenerated capacity.

E. Pressure Drop

Pressure-drop measurements were obtained using the apparatus depicted schematically in Figure 6. The source gas (dry compressed air) flow rate (1–10 L/min) was regulated by a rotameter and the pressure immediately upstream of the test sample was measured using a low-pressure diaphragm pressure gauge with a range of 0–10 inches of water.

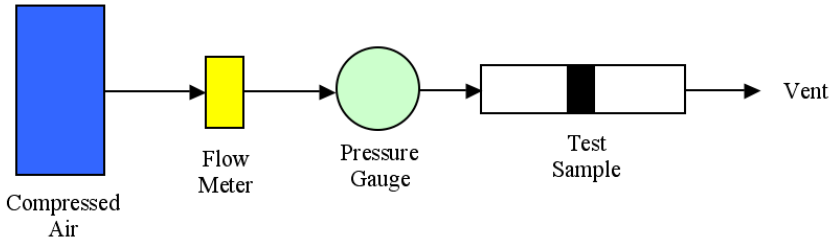

Figure 6. Schematic of experimental apparatus used for pressure drop measurements.

III. Results and Discussion

A. Carbon Characterization

The BET surface area of carbon microliths was found to be in the range 265–603 m^2/g, which was lower than we expected. PVDC carbon is known to be extremely microporous, with a BET surface area close to 1000 °C upon carbonization[5,6,17,20]. It was later found that the vitreous carbon foam used as a support for PVDC carbon did produce some weight loss upon sorbent carbonization and activation, which indicates that this material also contributed to the overall pore volume of the monolith. This is consistent with the nitrogen adsorption isotherm data, which showed that the percentage of micropore volume in monoliths was in the range 15–84%, again lower than we expected. It is still believed that the ammonia-sorption behavior determined in this study was largely dominated by the PVDC carbon in the monolith, but we also found that the nature of the carbon-foam support should be given more attention in future research. The total pore volume was between 0.27 cm^3/g and 1.06 cm^3/g, and the micropore volume was found to be in the range 0.10–0.23 cm^3/g. It is expected that increasing the degree of microporosity in future monoliths, e.g., by avoiding supports that contribute mesoporosity, will lead to improved performance.

B. Ammonia Sorption and Sorbent Regeneration

Numerous samples were fabricated and tested for ammonia adsorption and desorption. Table 1 summarizes the experimental details involved in the sample fabrication for a variety of representative samples, including the method of coating (solution vs. dry powder), the PVDC type, the maximum carbonization temperature and soak period, and the oxidation temperature and soak period (if employed). The table also provides the ammonia adsorption capacity measured for each sample. In some cases, adsorption data are included where additional sample conditioning (activation and/or oxidation) was employed. In addition to the foam samples, Table 1 also includes the results for three commercial granular carbons, including Ammonasorb II.

Table 1. Representative list of PVDC carbon-coated foam samples fabricated and tested. Test results for granular samples are also shown.

Sample ID	Coating Method	Precursor	Maximum Carbonization Temp, Period (°C, min)	Carbonized Mass (g)	Activated Mass (g)	Oxidation Temp, Period (°C, hours)	Adsorption Capacity (mg NH_3/g sorbent)		
							carbonized	activated	oxidized
04-29-11-e	Solution	Dow	1050, 240	0.632			0.093		
05-03-11-r	Solution	Dow	1050, 40	0.393	0.289			0.180	
05-03-11-w	Solution	Dow	1050, 40	0.437			0.112		
05-19-11-ab	Solution	Dow	1050, 40	0.929			0.144		
05-19-11-ai	Solution	Dow	1050, 40	0.903	0.621			0.143	
05-19-11-am	Solution	Dow	1050, 40	0.938		250, 24			0.533
06-14-11-bp	Solution	Solvay	1050, 40	1.023			0.010		
06-17-11-bq	Solution	Solvay	300, 75				0.105		
06-17-11-br	Solution	Solvay	1050, 40	1.025			0.004		
06-17-11-bt	Solution	Solvay	700, 240	1.069			0.053		
06-26-11-cc	Solution	Solvay	1050, 40	1.299	0.852			0.082	
06-26-11-ce	Solution	Solvay	1050, 40	1.046	0.774		0.018	0.083	
07-26-11-de	Dry Powder	Honeywell	900, 3	0.506		250, 24	0.669		6.107
08-08-11-di	Dry Powder	Honeywell	900, 3	0.519		250, 72	0.223		7.225
08-08-11-dj	Dry Powder	Dow	900, 3	0.412		250, 24	0.097		3.840
08-15-11-dl	Dry Powder	Honeywell	900, 3	0.59	0.607	250, 24		0.259	1.415
08-16-11-dm	Dry Powder	Honeywell	1450, 90	0.549		250, 24	0.027		0.098
08-16-11-dm	Dry Powder	Honeywell	1450, 90	0.549		325, 3			0.228
08-23-11-dr	Dry Powder	Honeywell	900, 3	0.634		250, 48	7.022		
09-09-11-ds	Dry Powder	Honeywell	800, 3	0.611		250, 24	6.465		
09-19-11-dv	Dry Powder	Honeywell	900, 3	0.489		325, 24	14.780		
Norit DARCO				1			1.959		
Calgon BPL				0.252			0.321		
Ammonasorb II				0.257			19.650		

Note that these measurements summarize the initial results for each sample under nominally dry conditions. Several foam samples, as well as the granular Ammonasorb II, were subjected to multiple adsorption cycles and testing after regeneration experiments (described below), under both dry and humid conditions.

Ammonia-sorption data can be presented in terms of either breakthrough curves or sorption-capacity curves, and these two different ways of presenting sorption data are illustrated in Figure 7. Although the information included in each of these curves is equivalent, most ammonia-sorption data have been reported in terms of sorption-capacity curves (e.g., see Ref. 3,4). In general, we will follow this convention, although in some cases breakthrough curves will also be shown to better illustrate whether or not ammonia concentration dropped to zero and for how long it stayed at the zero level.

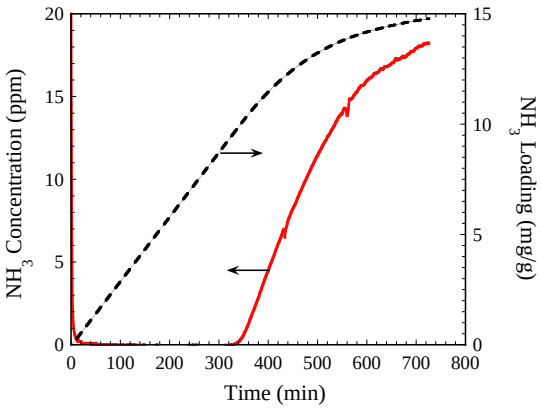

Figure 7. Ammonia breakthrough (left) and sorption-capacity (right) curves for carbon microlith sample 09-19-11-dv.

Sorbent Regeneration – Vacuum regeneration of TC sorbent is one of the most attractive features of AFR sorbents. Ammonia sorption on high-purity carbons that have not been impregnated with any acids is governed by physical adsorption (physisorption) rather than irreversible, or almost irreversible, chemisorption, which dominates ammonia sorption on acid-treated carbons. For this reason, little or no loss of sorption capacity is expected in our carbons following initial cycles of ammonia adsorption-desorption. In contrast, acid-treated carbons, such as Ammonasorb II, normally show little or no recovery of their original sorption capacity after the first chemisorption event.

This is in fact what was observed in a series of experiments involving PVDC/foam monolith 07-26-11-de, which was subjected to repeated ammonia adsorption-desorption cycles (Figure 8). It can be seen that the loss of sorption capacity is essentially limited to the first cycle, and that this loss is modest (about one third). In contrast, the loss of ammonia-sorption capacity in the case of acid-impregnated carbon Ammonasorb II is a factor of eight, which is shown in Figure 9. It should be noted that data in Figure 8 do not represent our best sorbent, but the one that has been most extensively studied with respect to multiple regeneration. Performance data in Figure 8 can be compared to the corresponding data for Ammonasorb II (Figure 9), and the superior regenerative capability of our monolithic sorbent is evident. It should be noted that Ammonasorb breakthrough curves do not even reach the zero level after the first adsorption experiment has been performed. This provides a clear contrast between our vacuum-regenerable sorbent and an acid-treated one (Ammonasorb II).

Another important result concerns the time needed for sufficient sorbent regeneration. Under the conditions used in this study, and for sorbent 07-26-11-de, we found that a room-temperature 15-minute exposure to vacuum resulted in a temporary and partial loss of ammonia-sorption capacity, i.e. incomplete desorption (compare lines 7 and 8 in Figure 8). This could easily be reversed upon a longer exposure of the spent sorbent to vacuum (see line 9 in Figure 8). It was also found that a one-hour exposure to vacuum at room temperature was sufficient to provide effective ammonia desorption (compare lines 7, 8, and 9 in Figure 8). Data in Figure 8 also show that this desorption time scale was shorter than the adsorption time scale (usually 70–90 minutes before breakthrough took place), which makes vacuum regeneration practical in a swing fashion. This is an important result proving the feasibility of vacuum regeneration of carbons that have pores with dimensions close to molecular scales (< 20 Å).

The Effect of Surface Oxidation – The strong effect of carbon oxidation on ammonia-sorption capacity is shown in Figure 10. It is evident that carbon exposure to ambient air results in a tremendous increase in ammonia-sorption capacity (up to a factor of 20, depending on oxidation exposure time and temperature). Moreover, it was found that sorption enhancement due to carbon oxidation is retained upon multiple vacuum regenerations of the sorbent (see Figure 8). These results can be explained by the formation of weakly acidic carbon-oxygen complexes resulting from oxygen chemisorption on carbon during oxygen pre-treatment. Apparently, the surface acidity is sufficient to increase ammonia-sorption capacity, but not strong enough to significantly impair ammonia desorption in the vacuum-regeneration step. The initial drop in ammonia-sorption capacity represented by the difference between line 1 and all the other lines in Figure 8 is almost certainly attributable to the presence of a small proportion (about one third) of strongly acidic sites. These tend to adsorb ammonia irreversibly. In the case of Ammonasorb II, which is a carbon impregnated with phosphoric acid, the carbon surface is composed of predominantly strong acidic sites, and this is why only about 12% of adsorbed ammonia can be vacuum-regenerated (see Figure 9).

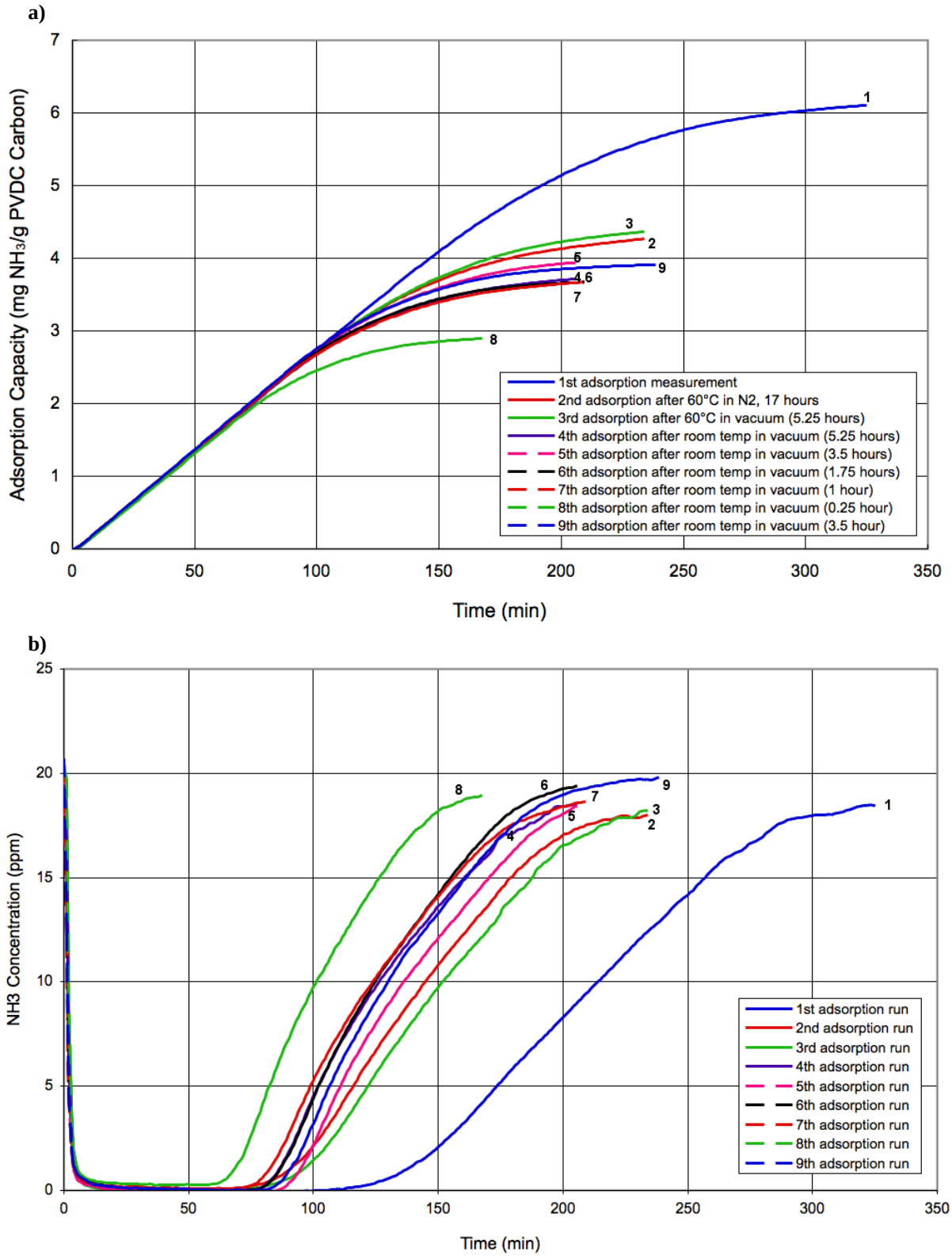

Figure 8. Ammonia sorption-capacity (a) and breakthrough (b) curves for carbon monolith sample 07-26-11-de oxidized at 250 °C and then subjected to multiple ammonia adsorption/vacuum-regeneration cycles.

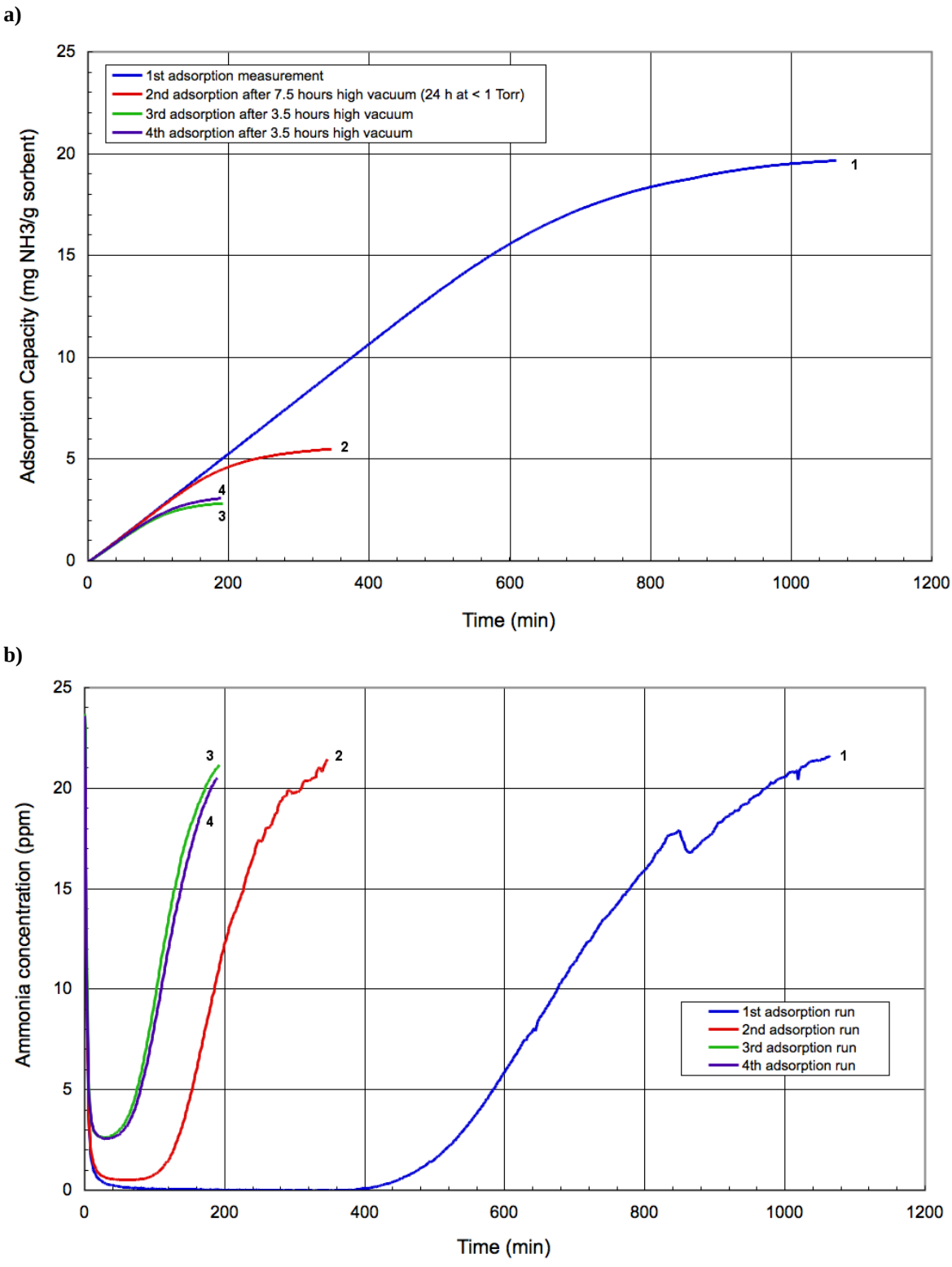

Figure 9. Ammonia sorption-capacity (a) and breakthrough (b) curves for acid-impregnated granular carbon Ammonasorb II that was subjected to multiple ammonia adsorption/vacuum-regeneration cycles.

a)

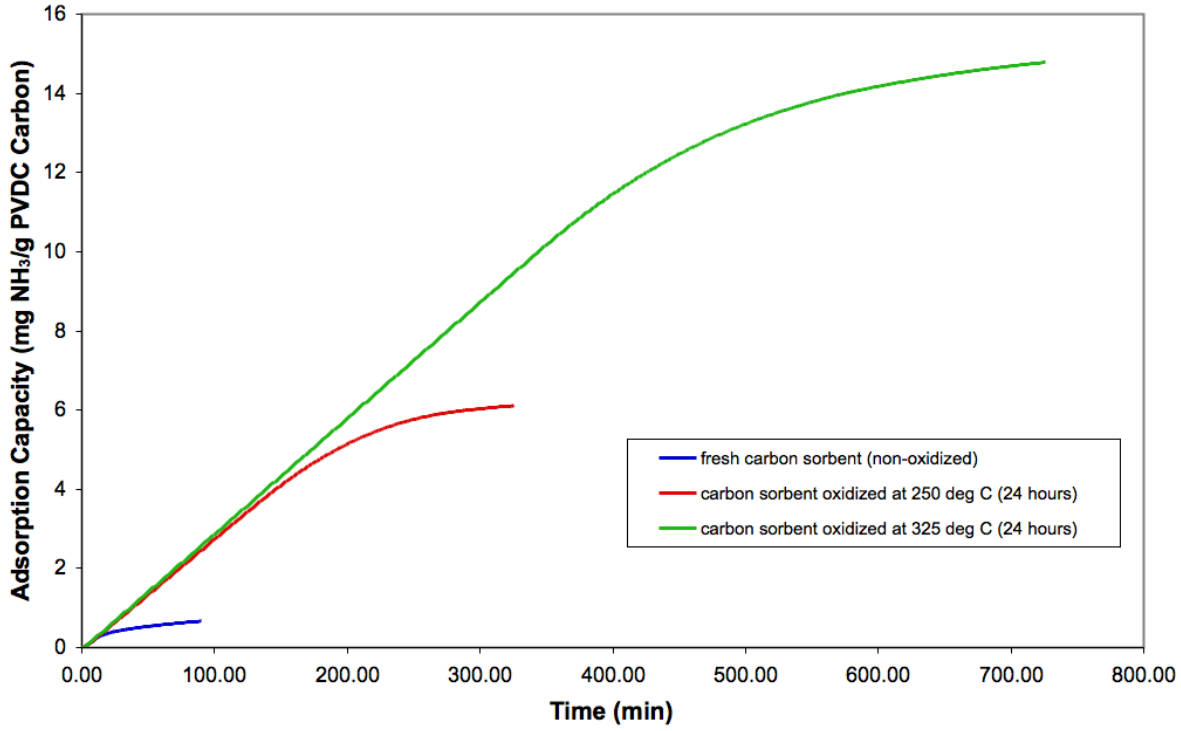

b)

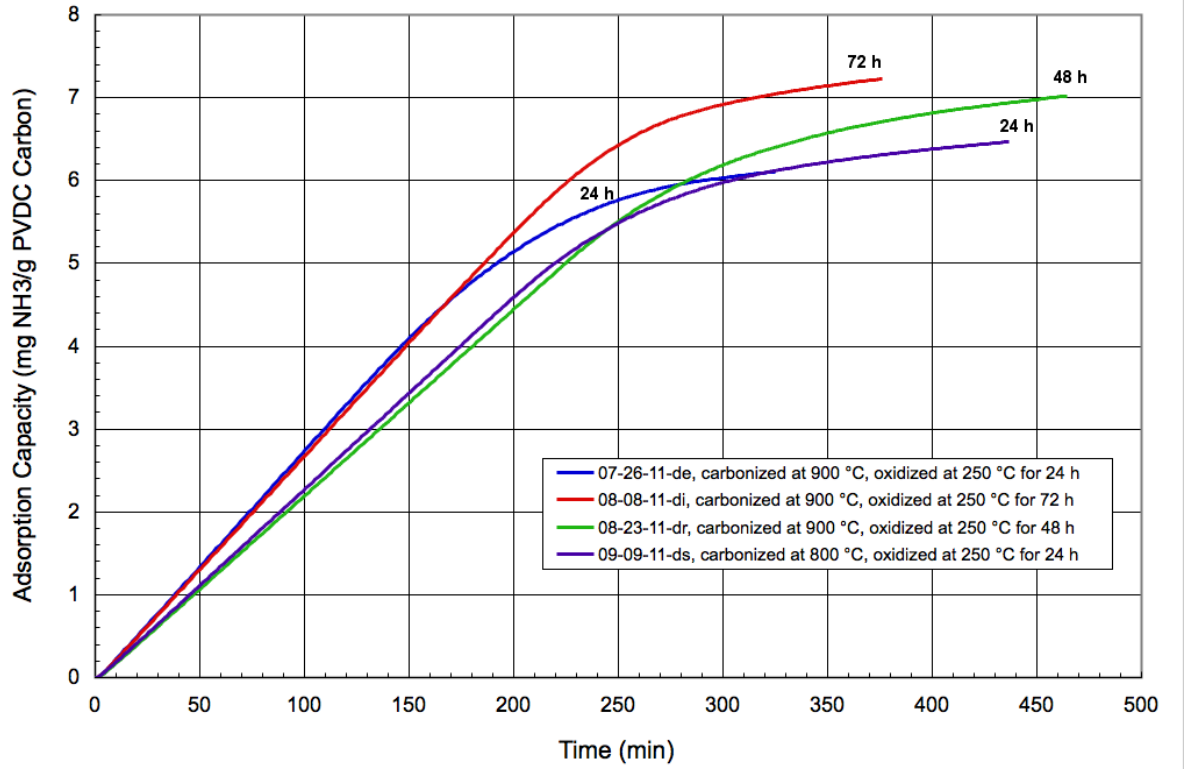

Figure 10. Ammonia sorption-capacity for freshly prepared (unoxidized) carbon monoliths that have been oxidized at various temperatures (a) and at various exposure times at 250 °C (b).

The Effect of Gas Humidity – Like most of the data published in the literature, our initial experiments involved ammonia sorption from a flow of dry gas. It was believed that the effect of gas humidity was only modest for activated carbons (~25% for 40% relative humidity), as reported in Ref. 3 and 4. We were pleasantly surprised when experiments with humid gas showed that our sorbents' performance was improved by a factor of ~2.5 when inlet gas contained water vapor in addition to ammonia, oxygen, and nitrogen. These results are summarized in Figure 16. Following discussions with NASA Johnson Space Center scientists, we decided to include lower humidity levels (10%) in our study. Such low humidity seems be relevant to the PLSS operation in view of the recent NASA data that indicate extremely effective moisture removal taking place in the CO_2-control unit.

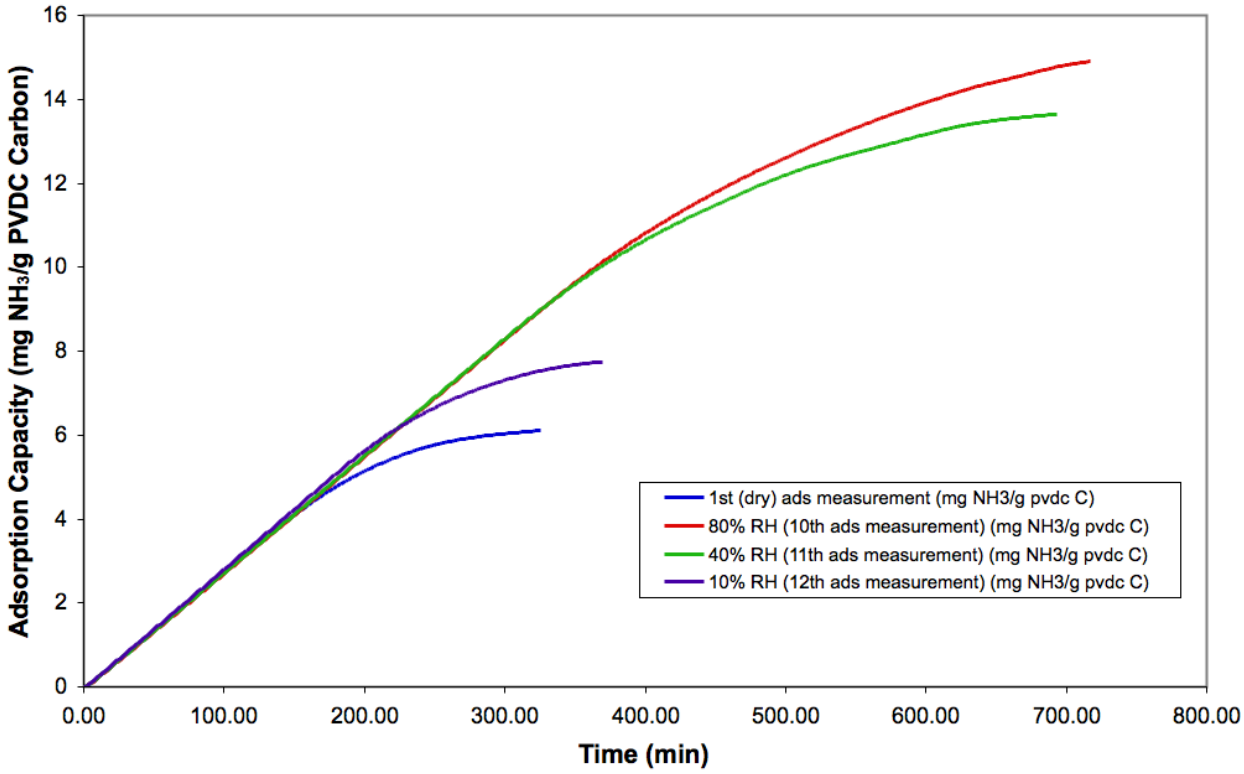

Figure 11. The effect of gas relative humidity (RH) on ammonia-sorption performance for carbon monolith 07-26-11-de.

The Effect of Carbon Activation – Since carbon-activation causes profound changes in the carbon pore structure (pore-size distribution, specific surface area, pore volume, etc.), it is not surprising that these changes should be reflected in ammonia-sorption performance data. An example of sorption-capacity curves for a carbon monolith derived from PVDC is shown in Figure 12. A strong effect of carbon activation is evident in this case, but the magnitude of sorption enhancement (or reduction) depends on the nature of the carbon, its precursor, carbonization conditions, activation agent (CO_2, steam, oxygen), and activation conditions (temperature and hold time). A systematic study of the effect of the above variables on ammonia sorption was beyond the scope of this project.

The Effect of Carbon Precursor – Three types of PVDC were used, and they were obtained from different suppliers: Dow, Solvay, and Honeywell. The first two are commercial products that include some co-polymers and additives, whereas the Honeywell PVDC is a high-purity research grade. Carbons prepared from the above precursors showed different performance characteristics, and monoliths from some of them were easier to fabricate than from others. In general, the Honeywell PVDC carbon showed better sorption capacity than Dow carbon, which in turn was better than Solvay. Polymer solubility and the effect of carbon-surface oxidation should also be taken into account. A systematic study of the effect of polymer precursor is certainly warranted.

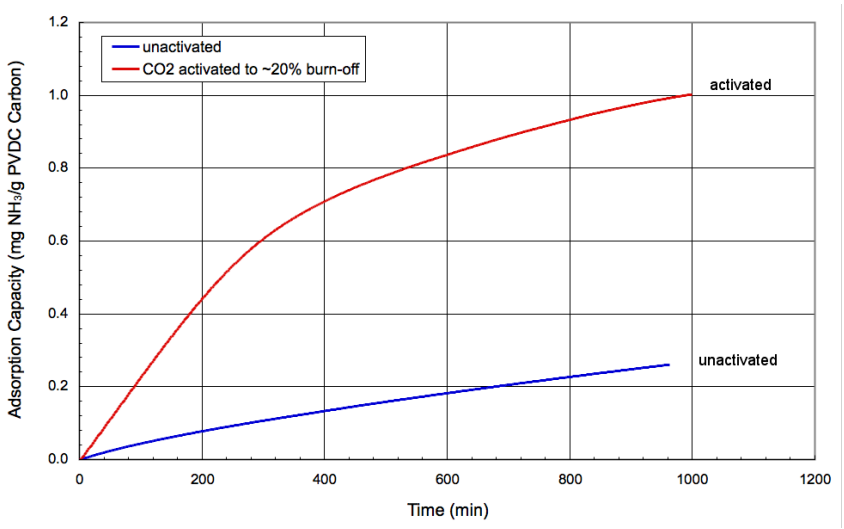

Figure 12. The effect of carbon activation on ammonia-sorption capacity (a PVDC-derived carbon monolith with 121 parallel channels).

Comparison with Off-the-Shelf Granular Activated Carbons – Side-by-side comparisons were conducted with three commercial carbons: Calgon Ammonasorb II (impregnated with phosphoric acid), Calgon BPL (no acid impregnation or acid washing), and Norit DARCO (acid-washed). The comparison of monolithic carbon with the state-of-the-art Ammonasorb II is shown in Figure 8 and Figure 9, and the monolithic carbon clearly wins because of its regenerability and good sorption capacity. Ammonia-sorption capacity for our monolithic carbons was found to be generally a factor of 10 better than for Calgon BPL, and a factor of 2 better than Norit DARCO.

C. Pressure Drop

Pressure-drop measurements were performed for some of our foam-based monoliths, and Figure 13 shows the comparison of our data with the calculated pressure drop for a corresponding packed-bed of granular sorbent. The advantage of the monolith over a packed bed seems to be at least a factor of two, and a difference of about two orders of magnitude was found for monoliths with parallel channels[17,18].

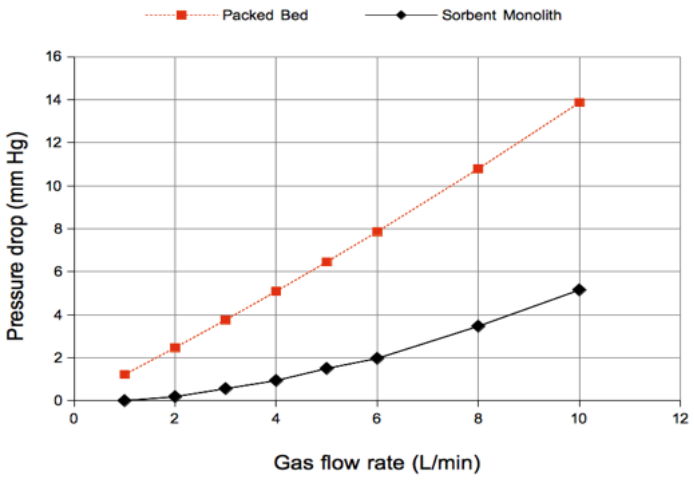

Figure 13. Comparison of pressure drop over a carbon monolith with the corresponding packed bed of granular sorbent. The measurements were performed on a 22 mm ID foam-based monolith, which was 6 cm in height. The weight of carbon was 4.62 g. For the packed bed, the pressure drop was calculated using the Ergun equation[21], assuming the same bed diameter and sorbent weight, a height of 2.1 cm, a bed voidage of 40%, and a particle size of 0.3 mm.

D. Resistive Heating

It has been shown experimentally that resistive heating to about 80 °C is rapid and effective in the case of carbon-sorbent monoliths. This was done by connecting electrodes to opposite ends of a Duocel vitreous carbon foam and applying AC voltage. The temperature of the carbon foam was monitored using a hand-held pyrometer. It was demonstrated that the temperature could easily reach about 80 °C within less than 30 seconds.

IV. Conclusions

The main findings of the study are listed below.

- Numerous carbon sorbent monoliths were fabricated and tested.
- Reproducible regeneration by exposure to vacuum for about 1 hour at room temperature was demonstrated throughout multiple adsorption-desorption cycles.
- Using an ammonia-sorption capacity of 8 mg/g sorbent and an ammonia-generation rate of 83 mg per 8 hours, it can be shown that the sorbent weight can be reduced from the current 454 g to ~11 g for an 8-hour EVA that involves no TC-sorbent regeneration. For EVAs involving pressure-swing TC Control System (TCCS) operation, only about 3 g of carbon is needed if a sorption-regeneration cycle time is 1 hour.
- A comparison of ammonia-sorption capacity for our best sorbent with the corresponding data for Ammonasorb II, the currently used state-of-the-art carbon is shown in Figure 14. The superior performance of the monolithic carbon with respect to sorbent regeneration is evident.
- Effective carbon surface conditioning via oxidation was demonstrated that enhances ammonia sorption without impairing sorbent regeneration.
- Depending on the particular sorbent monolith geometry, the reduction in pressure drop, and thus also power requirement, with respect to granular sorbent is estimated to be between 50% and two orders of magnitude.
- It was shown that the carbon sorbent monolith could be resistively heated by applying voltage to the opposite ends of the monolith.

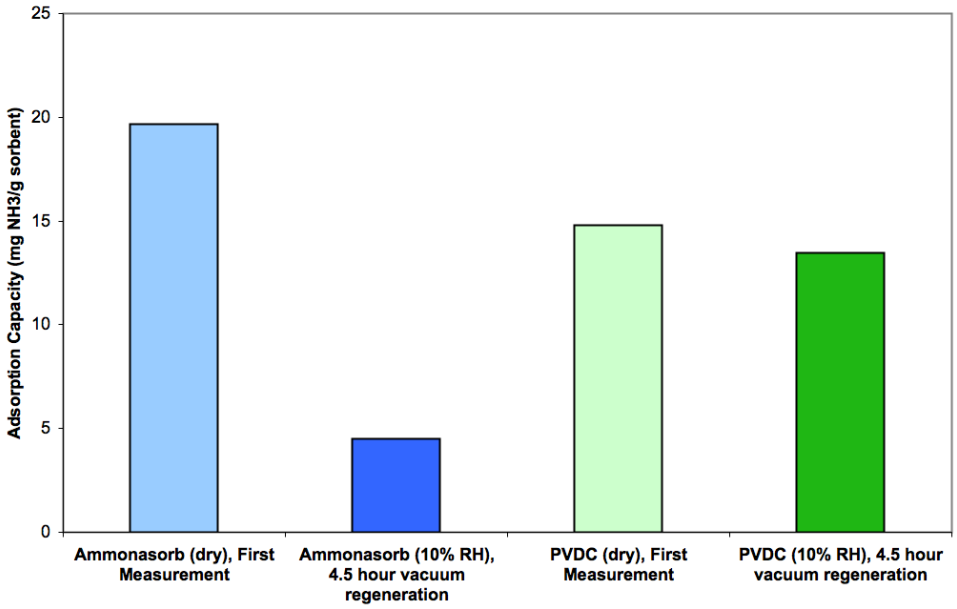

Figure 14. The effect of vacuum regeneration on ammonia-sorption capacity for the state-of-the-art acid-impregnated activated carbon (Ammonasorb II) and one of the carbon monoliths studied (highly porous carbon supported on high-strength carbon foam). Good sorbent regeneration is evident for the monolithic carbon, and its ammonia-sorption capacity after regeneration is almost 3 times higher than for Ammonasorb II. Note that data were collected at low relative humidity (RH) conditions (10%).

Acknowledgments

The authors wish to thank the National Aeronautics and Space Administration (NASA) for financial support under Contract No. NNX11CG26P.

References

[1]Paul, H. L. and Jennings, M. A., "Results of the trace contaminant control trade study for space suit life support development," Proc. 39th Int. Conf. on Environmental Systems (ICES), Savannah, Georgia, July 12-16, 2009, SAE technical paper No. 2009-01-2370, SAE International, 2009.

[2]http://en.wikipedia.org/wiki/Activated_carbon

[3]Luna, B., Podolske, J., Ehresmann, D., Howard, J., Salas, L. J., Mulloth, L., and Perry, J. L., "Evaluation of commercial off-the-shelf ammonia sorbents and carbon monoxide oxidation catalysts," *Proc. 38th Int. Conf. on Environmental Systems (ICES)*, San Francisco, California, June 29-July 2, 2008, SAE technical paper No. 2008-01-2097, SAE International, 2008.

[4]Luna, B., Somi, G., Winchester, J. P., Grose, J., Mulloth, L., and Perry, J., Evaluation of commercial off-the-shelf sorbents and catalysts for control of ammonia and carbon monoxide," *Proc. 40th Int. Conf. on Environmental Systems (ICES)*, Barcelona, Spain, July 11-15, 2010, AIAA technical paper No. 2010-6062, AIAA, 2010.

[5]Wójtowicz, M.A., Serio, M.A., Smith, W. and Simons, G.A., *Gas Storage Using Microporous Carbons*, Final Report, NASA Phase 1 SBIR contract No. NAS9-19470, Advanced Fuel Research, East Hartford, CT, 1996

[6]Wójtowicz, M.A., Bassilakis, R., Leffler, M., Serio, M.A., Simons, G.A., Fuller, W., *Gas Storage Using Microporous Carbons*, Final Report, NASA Phase 2 SBIR contract No. NAS9-97012, Advanced Fuel Research, East Hartford, CT, May 2000.

[7]Wójtowicz, M. A., Markowitz, B. L. and Serio, M. A., "Microporosity development in carbons for gas-storage applications," a keynote lecture, EUROCARBON '98, Strasbourg, France, 5-9 July, 1998; *Proc. EUROCARBON '98: Science and Technology of Carbon*, AKK & GFEC, Strasbourg, France, pp. 589-590.

[8]Wójtowicz, M. A., Markowitz, B. L., Smith, W. W. and Serio, M. A., "Microporous carbon adsorbents for hydrogen storage," an invited keynote lecture, *Proc. Third International Conference on Materials Engineering for Resources (ICMR '98)*, Akita, Japan, 26-28 October, 1998, pp. 416–429.

[9]Wójtowicz, M. A., Markowitz, B. L., Bassilakis, R. and Serio, M. A., "Hydrogen storage carbons derived from polyvinylidene chloride," a poster presented at the 1999 Hydrocarbon Resources Gordon Research Conference, Ventura, CA, 17-22 January, 1999; an award for an outstanding paper.

[10]Wójtowicz, M. A., Smith, W. W., Serio, M. A., Simons, G. A., and Fuller, W. D., "Microporous carbons for gas-storage applications," *Proc. Twenty-Third Biennial Conference on Carbon*, the Pennsylvania State University, July 13–18, 1997, vol. I, pp. 342-343

[11]Simons, G. A. and Wójtowicz, M. A., "A model for microporosity development during char activation," *Proc. Twenty-Third Biennial Conf. on Carbon*, Pennsylvania State University, July 13–18, 1997, vol. I, pp. 328-329

[12]Simons, G. A. and Wójtowicz, M. A., "Modeling the evolution of microporosity and surface area during char activation," *Proc. 9th Int. Conf. on Coal Science* (A. Ziegler, K. H. van Heek, J. Klein and W. Wanzl, Eds.), DGMK, Hamburg, Germany, 1997, pp. 1783-1786

[13]Simons, G. A. and Wójtowicz, M. A., "Modeling the evolution of microporosity in a char-activation process involving alternating chemisorption-desorption cycles," *Proc. EUROCARBON '98: Science and Technology of Carbon*, AKK and GFEC, Strasbourg, France, 5-9 July, 1998, pp. 273-274.

[14]Wójtowicz, M. A., Markowitz, B. L., Smith, W. W. and Serio, M. A., "Microporous carbon adsorbents for hydrogen storage," *Int. Journal of the Society of Materials Engineering for Resources* **7** (2), 253–266, 1999

[15]Wójtowicz, M. A., Markowitz, B. L., Simons, G. A. and Serio, M. A., "Gas-storage carbons prepared by alternating oxygen chemisorption and thermal desorption cycles," *ACS Div. of Fuel Chem. Prepr.* **43** (3), 585-590, 1998

[16]Wójtowicz, M. A., Bassilakis, R., Leffler, M. P., Serio, M. A. and Fuller, W. D., "Adsorption of hydrogen on activated carbons derived from polyvinylidene chloride," *Proc. First World Conf. on Carbon EUROCARBON 2000*, Berlin, Germany, 9-13 July, 2000, vol. I, pp. 407–408.

[17]Wójtowicz, M. A., Florczak, E., Kroo, E., Rubenstein, E., Serio, M. A., and Filburn, T., *Carbon-Supported Amine Monoliths for Carbon Dioxide Removal*, Final Report, NASA Phase I SBIR contract No. NAS9-03012, Advanced Fuel Research, East Hartford, CT, July 2003.

[18]Wójtowicz, M. A., Florczak, E., Kroo, E., Rubenstein, E. P., Serio, M. A., and Filburn, T., "Monolithic sorbents for carbon dioxide removal," *Proc. 36th Int. Conf. on Environmental Systems (ICES)*, Norfolk, Virginia, July 17-20, 2006, SAE technical paper No. 2006-01-2193, SAE International, 2006.

[19]Wójtowicz, M. A., Florczak, E., Kroo, E., Rubenstein, E., Serio, M. A., and Filburn, T., *Carbon-Supported Amine Monoliths for Carbon Dioxide Removal*, Final Report, NASA Phase 2 SBIR contract No. NNJ04JA15C, Advanced Fuel Research, East Hartford, CT, December 2006.

[20]Walker, P. L., Jr., Austin, L. G., and Nandi, S. P., "Activated Diffusion of Gases in Molecular-Sieve Materials," in *Chemistry and Physics of Carbon*, P. L. Walker, Jr. (Ed.), vol 2, Marcel Dekker, New York, 1966

[21]Ergun, S., *Chem. Eng. Progr.* **48**, 89–94 (1952).